DNA sequencing, microbial sensors, and the discovery of buried mineral resources

Rachel L. Simister[1,2], Bianca P. Iulianella Phillips [2,3], Andrew P. Wickham[2,3], Erika M. Cayer[2,3], Craig J.R. Hart [2,3], Peter A. Winterburn [2,3]† and Sean A. Crowe [1, 2] *

1. Department of Microbiology & Immunology, University of British Columbia, Vancouver, BC, V6T 1Z3, Canada
2. Department of Earth, Ocean and Atmospheric Sciences, University of British Columbia, Vancouver, BC, V6T 1Z3, Canada
3. MDRU-Mineral Deposit Research Unit, Department of Earth, Ocean and Atmospheric Sciences, University of British Columbia, Vancouver, BC, V6T 1Z3, Canada

† Deceased
* Corresponding author

Twitter handles:
@crowe_lab
@RachelSimister

DNA sequencing, microbial sensors, and the discovery of buried mineral resources

Rachel L. Simister[1,2], Bianca P. Iulianella Phillips [2,3], Andrew P. Wickham[2,3], Erika M. Cayer[2,3], Craig J.R. Hart [2,3], Peter A. Winterburn [2,3]† and Sean A. Crowe [1, 2] *

1. Department of Microbiology & Immunology, University of British Columbia, Vancouver, BC, V6T 1Z3, Canada
2. Department of Earth, Ocean and Atmospheric Sciences, University of British Columbia, Vancouver, BC, V6T 1Z3, Canada
3. MDRU-Mineral Deposit Research Unit, Department of Earth, Ocean and Atmospheric Sciences, University of British Columbia, Vancouver, BC, V6T 1Z3, Canada

† Deceased

* Corresponding author

Correspondence to Sean A. Crowe: sean.crowe@ubc.ca

Abstract

New mineral resources are critical to both sustaining human population growth and technological improvements that will enable global decarbonization. New and innovative exploration technologies that enable detection of deeply buried mineralization and host rocks are required to meet these demands. Here we show that DNA amplicon sequencing of soil microbial communities resolves anomalies in microbial community composition and structure that reflect the surface expression of kimberlite ore bodies buried under 10s of meters of overburden. Indicator species derived from laboratory amendment experiments were employed in an exploration survey in which the species distributions effectively delineated the surface expression of buried kimberlites. Additional indicator species derived from field observations improved the blind discovery of kimberlites buried beneath similar overburden types. Application of DNA sequence-based analyses of soil microbial communities to mineral deposit exploration provides a powerful illustration of how the sensing capabilities of environmental microbial communities can be leveraged in the discovery of critical new resources.

Introduction

Microorganisms operate together with geological processes to drive biogeochemical cycles that shape Earth's surface chemistry and climate through time [1]. They interact with minerals at the nano- to micro-scales [2], and these interactions give rise to emergent properties across the multiple-scales that characterize the biosphere [3]. Through billions of years of evolution, microorganisms have honed their ability to sense and interact with their surrounding environments and, in particular, to respond to the availability of mineral nutrients and substrates. Microbial community compositions and structures are thus sensitive reflections of their habitats [4-6] and analyses of microbial communities can provide a wealth of information on their surrounding environments.

High-throughput sequencing technologies now allow us to analyse microbial communities and leverage microbial sensing to interrogate the environment with unprecedented sensitivity and resolution [7-9]. Sequence based microbial community analyses, for example, have been used to sense organic and inorganic contaminants in groundwater at the watershed-scale [7]. More broadly, microbial communities are known to respond to a wide-range of physical-chemical properties including pH [10], salinity [11], temperature [12, 13], wind, light intensities [14] and mineral micronutrients [15]. To date, however, we have mostly overlooked the potential power of microbial sensors to enable discovery in the natural environment and are only just beginning to harness the capacity of environmental microbial communities to help meet human needs. As the human population grows and modernizes, for example, its demand for mineral resources is rapidly increasing, but at the same time, existing mineral deposits are becoming exhausted and the frequency of new deposit discovery is declining [16-18]. New demand for mineral resources must, therefore, be increasingly met through discovery and development of deeply concealed deposits [19-21] and this is where microbial sensors could play an important role.

Innovation and the development of new tools and techniques are needed to improve our ability to find mineral resources. It has been known for more than half a century that vegetation responds to subsurface geologic features, presumably through the subtle influence of bedrock geology on the physical and chemical properties of surface soils [22, 23]. The link between vegetation patterns and bedrock geology prompted early use of biological surveys in mineral deposit exploration [24-26]. Vegetation patterns, however, are confounded by many variables [27, 28], and thus rarely offer clear indications of buried mineral deposits. Use of biological surveys in exploration has been extended to soil microbial communities [29-33], but the complexity of these communities is intractable through the approaches of classical microbiology, while early generation molecular approaches lacked throughput [34-36]. Now, however, even the most complex microbial communities, like those found in soils, can be resolved through semi-quantitative to quantitative sequence-based analyses [10, 37, 38]. Given that every gram of soil contains thousands of microbial taxa [39, 40], each housing hundreds to thousands of genes sensing and interacting with the surrounding soil environment [41, 42], the power of this approach to identify anomalies in soils is unprecedented. We show that rock units and mineral deposits buried under 10s of meters of soil and unconsolidated surficial materials can be located at the surface through microbial community profiling using high-throughput DNA amplicon sequencing.

Results and Discussion

Microbial community responses to ore materials

Incubation experiments reveal that microbial community compositions and structures respond directly to amendments with ground rock from diamondiferous kimberlites. We amended tundra-derived soils with pulverized (80% passing 10 mesh (2 mm)) kimberlite (5 % w/w) and analysed the response of soil microbial communities through amplicon sequencing of the small subunit (16S) ribosomal rRNA gene.

Kimberlites are variably serpentinized, high-Mg ultramafic rocks that are host ores of natural gem and industrial quality diamonds and are increasingly considered as source materials for atmospheric carbon capture and storage technologies [43, 44]. At 5%, amendment with kimberlite had a nominal effect on overall soil chemical composition (Table S5). Baseline soils had microbial community compositions comprised predominantly of 6 phyla—Proteobacteria, Actinobacteria, Bacteroidetes, Acidobacteria, Chloroflexi and the WPS-2 candidate phylum (Fig. 1a, b). The soils also contained appreciable, but lesser, proportions of Verrucomicrobia, Planctomycetes and Gemmatimonadetes (Fig. 1a). Such community compositions are typical of both tundra soils [45-47] and a broad suite of soils, more generally [38]. We found that over a period of 85 days, the microbial community composition and structure in amended soils diverged from the baseline with pronounced changes observed at the phylum level, including increases in the abundances of Proteobacteria and Bacteroidetes from 46% to 68% and 6% to 16%, respectively, in response to amendment (Fig. 1a, b). Four phyla (Chloroflexi, Acidobacteria, Actinobacteria and WSP-2), on the other hand, decreased (from 6%, 5%, 19%, 7% in the baseline to 1%, 2%, 8%, 1%, following amendment, respectively) (Fig. 1a, b). Experimental results thus reveal that the addition of kimberlite to tundra-derived soils causes strong shifts in microbial community composition that are easily resolved through amplicon sequencing of the 16S rRNA gene.

Amendment with kimberlite material was sufficient to cause appreciable changes to microbial community structure and a decline in diversity at the species level (97% sequence identity in the 16S rRNA gene), relative to the baseline. Diversity indices like Chao1, for example, show a decrease in species richness from 1610 ± 70 in the baseline soils to 830 ± 60 following amendment (Table S1). This decline in species richness is also supported by a decline in the number of observed OTUs, which decrease by 48% (on average 990 ± 10 in control samples, and 520 ± 10 in kimberlite amended soils) (Fig. 1c,

Table S1). Reduction in species richness in response to amendment is likely due both to selective growth of some taxa and the death and decay of others. This is consistent with limited overall community growth during the incubations based on qPCR assays of 16S rRNA gene abundance (S-Fig. 1). Differences in microbial community composition and structure between baseline and amended soils were evaluated through hierarchical-clustering analysis (Fig. 1e). All baseline soils clustered tightly, exhibiting both similar bacterial diversities and microbial community compositions, whereas amended soils grouped separately. This confirms that kimberlite amendment induced clear and reproducible shifts in microbial community compositions, demonstrating that major features of soil microbial community compositions and structure are sensitive to the presence of kimberlite materials on timescales of several weeks.

Beyond high-level changes in the taxonomic composition and structure, many individual species responded to ore amendment. An indicator species analysis (Table S4 a,b) revealed a total of 375 species that responded significantly (Linear Discriminant analysis (LDA) threshold score >2) to kimberlite amendment, and thus qualify as indicators for kimberlite material. Of these, 65 species (17%) increased in abundance over the 85-day incubation period, whereas 310 species (83%) decreased in relative abundance, with respect to the baseline (Table S4 a, b, Fig. 1d). Notable examples of species that increased in abundance include *Sphingomonas sp., Janthinobacterium sp.,* and *Pedobacter sp*., whereas species that decreased include *Nevskia sp., Mucilaginibacter* and *Conexibacter sp*., (Table S4 a, b, Fig. 1d). Collectively, the 65 species that increased in abundance following amendment made up 60% of the total community following incubation, relative to 0.6% in the baseline. Following incubation, these 65 species exhibited a mean of 1% and median of 0.2% in amended soils, versus 0.01 and 0 % in the baseline, respectively. Similarly, the 310 species that decreased in abundance following amendment made up 8% and 74% of the total community in amended and baseline soils, respectively. These species exhibited a

mean of 0.027% and median of 0.007%, versus 0.24% and 0.065% in amended versus baseline soils, respectively, following incubation. These results thus demonstrate that amendment with kimberlite induces a fundamental reorganization of generally low abundance microbial community members with the overall effect of entirely changing the microbial community composition in a matter of a few weeks. Furthermore, amendment with kimberlite selects for ingrowth of members of the rare biosphere, that were mostly undetectable prior to incubation, to abundances of several % (e.g. *Janthinobacterium sp*), whereas other members dropped from several percent, to obscurely low abundances (e.g. *Nevskia sp*) (Table S4 a,b, Fig. 1d). This demonstrates that microbial communities are exquisitely sensitive and responsive to subtle variations in the mineral composition of soils with strong potential to act as sensors of this variation in the environment.

Microbial community profiling over buried mineralization

Tundra soils analysed over buried diamondiferous kimberlite mineralization in northern Canada (Northwest Territories) reveal largely homogenous microbial community compositions, but also differences in diversity that are spatially related to the surface expression of the underlying kimberlite (Fig. 2b). The B-horizons of soils that developed on up to 20 m thick glacial tills were sampled in a grid pattern across the surface expression of a kimberlite body that has been well defined by drilling (kimberlite DO-18) (S-Fig. 3a). The surface materials are dominated by till in the northern section of the sampled area and till, glaciolacustrine clay, glaciofluvial silt, sand, gravel, and organic deposits in the south. Most soil microbial-community members belong to the Proteobacteria, Acidobacteria, Verrucomicrobia, and Actinobacteria phyla (Fig. 2a), which is comparable to the dominant phyla in the soils used in our incubation experiments, soils from other tundra environments [45-47], and soils globally [39, 41]. The number of species observed ranges from 497-2025 with a mean of 1400 +/-300 and estimates of total

159 species richness (Chao1) range from 737-3306 with a mean of 2300 +/- 580, implying that these soils have
160 diversity typical of other soils, which can range from 100's to thousands of observed species per sample
161 (Table S2,3) [39, 48]. Furthermore, estimates that also consider community evenness (Inverse Simpson)
162 imply that species abundances are not evenly distributed in these soils (inverse Simpson indexes range
163 from 16-131, with a mean of 72 +/- 29) (Table S2,3). When these soils are grouped according to their
164 spatial relationships to the surface expression of the kimberlite body, we find that microbial species
165 richness in soils directly overlying the kimberlite is, on average, 29% lower than that in the background
166 soils (average chao1 index of 1840 ± 80 above surface projection of the kimberlite and 2600 ± 100 above
167 background), which are geographically removed from the underlying kimberlite (Fig. 2b). Whereas
168 differences in community structure reflect proximity to buried kimberlite, high-level community
169 compositions do not appear sensitive to buried kimberlite mineralization, and the abundances of the major
170 microbial phyla are similar across the entire sampling grid (Fig. 2a).

171 Differences in microbial community compositions of soils situated directly above the surface
172 expression of kimberlite, and those of background soils can be observed through statistical analyses
173 conducted at the species level. Hierarchical clustering analyses demonstrate that soils situated above
174 buried mineralization have microbial communities that are more similar to each other than they are to the
175 background soil communities. Several clusters had more than 50% of soils located above the surface
176 expression of the kimberlite (clusters 1, 4, and 5), whereas some clusters only contained background soils
177 (clusters 2, 3, 6, and 7) (Fig. 2c). This implies that though high-level differences in phyla, like those
178 observed in the incubation experiments, may not be expressed in natural settings, there are more subtle
179 differences in community composition that are resolvable through more nuanced analyses.

180 Species level fingerprints identified through indicator species analyses successfully resolve soils
181 that overlie buried kimberlite. Of the 65 indicator species identified through the incubation experiments,

59 were present in soils surveyed around the DO-18 deposit. 19 of these indicators, furthermore, were appropriately enriched in soils overlying the buried mineralization, relative to the background, and thus effectively resolve the surface expression of the kimberlite (Fig. 2e). We also conducted an indicator species analysis by comparing microbial communities overlying the surface expression of the deposit to those from background soils and this yielded a further 59 indicator species, 2 of which were the same as those identified through incubations (Table S4). Albeit small (3%), the overlap in indicator species between the incubation soils and the soils from DO-18 suggests that collections of indicator species can be more broadly extensible, at least across similar types of mineralization, and in comparable soil terrains. Combining the field-based indicator species with those from the incubation experiments yields a collected set of 78 indicators and generation of anomaly maps with this combined indicator set very effectively resolves the underlying kimberlite (Fig. 2f). For comparison we have also employed commonly used geochemical kimberlite pathfinder elements including Cr, Ni, Mg, and Nb (Fig. 2g). These pathfinders display an anomaly pattern that indicates glacial transport of kimberlite material away from the bedrock source and yields responses that are geographically less precise and quantitatively less pronounced (Fig. 2d) than the microbial indicators. Comparing the response ratios for geochemical and microbiological indicators it becomes immediately evident that DNA sequence based microbial community profiling much more effectively resolves the location of buried kimberlite mineralization than the geochemical data and suggests that amplicon-based microbial community profiling provides a robust and surgical mineral exploration tool.

Application of microbial community profiling to blind discovery of buried mineralization

As a proof of-concept, we used microbial indicators derived from our incubation experiments and analyses of DO-18 soils to resolve kimberlite mineralization at another location (Kelvin) in the Northwest

Territories (S-Fig. 2). The Kelvin kimberlite is overlain approximately 4 m of glacial till, and up to 150 m of bedrock cover the underlying kimberlite deposit (S-Fig. 3 b, c). Soils here are composed of poorly sorted clay, silt, sand, gravel, as well as dispersed boulder fractions (diamicton). As with DO-18, phylum level distributions were relatively homogenous across the sampling grid, but variability was observed at the species level and this variability could be geographically linked to the surface expression of the buried kimberlite (Fig. 3 a, b, c, e, f).

The application of our combined suite of 78 indicator species developed through both incubation experiments and statistical analyses at DO-18 led to anomaly delineation that precisely resolved the geographic location of the underlying kimberlite mineralization at Kelvin (Fig. 3e). Again, for comparison, we also analysed a suite of geochemical indicators (Nb, Cr, Ni, Mg), which yielded erratic anomalies that are discordant with the surface expression of the underlying kimberlite (Fig. 3 d, g). Therefore, like at DO-18, DNA sequence-based microbial community profiling at Kelvin more effectively resolves buried mineralization than geochemical analyses. Application to Kelvin, furthermore, demonstrates that microbial community indicators developed at one deposit can be applied to the discovery of other deposits, at least in the same soil terrains or ecoregions. It further implies that the development of databases of indicator species can improve the use of microbial community profiling as an exploration tool. To illustrate this point, we conducted an indicator species analysis for Kelvin, as we did for DO-18 above, and this yields and additional 8 indicator species, of these one is common to DO-18 (Fig. 3f). Our analyses at Kelvin thus demonstrate capacity for blind discovery of kimberlite mineralization buried under 10s of meters of overburden using DNA sequencing based microbial community analyses. These analyses can be used as a means for effectively defining drill targets in deposit to regional-scale phases of mineral exploration.

Our demonstration that DNA sequences from soil microbial communities effectively resolve buried mineralization illustrates how modern sequencing technology can be leveraged to access microbial sensors in the environment. This finding, foremost, shows that DNA sequencing of soil microbial communities can be used in the discovery of new mineral deposits, which, by analogy to the development and widespread application of geochemical tools to mineral exploration in the 1970's, may catalyze new deposit discovery in the decades to come. This has potential to promote the discovery of new kimberlite bodies, which could be utilized as source rocks for atmospheric carbon sequestration as well as for their stores of gem and industrial grade diamonds. DNA sequencing of soil microbial communities also has potential application across a broad array of metallic deposits, like porphyry-type copper deposits, for which the greatest mineral potential exists in terrains with thick cover such as northern Chile and British Columbia, Canada. This should be tested through further research. More broadly, that microbial community compositions can provide better resolved indicators of subsurface geology than geochemical analyses underscore the idea that microorganisms are acutely sensitive to their surroundings and respond to parameters that may themselves be only poorly resolved through use of even our most sophisticated existing analytical tools. Use of DNA sequences from microbial communities as vectors towards buried ore mineralization represents a powerful example of how such microbial information may become essential for sustaining human populations and resulting resource demand.

Data availability

Sequences were deposited into the Sequence read archive (SRA) under accession number PRJNA698256.

Acknowledgments

Support for this work came from NSERC/AcmeLabs/Bureau Veritas Minerals Industrial Research Chair in Exploration Geochemistry held by PAW and a Tier II Canada Research Chair in Geomicrobiology held by SAC. The research was further supported by an NSERC Discovery grant (0487) held by SAC. The Government of the Northwest Territories (GNWT) provided in-kind financial support and Barrett Elliott (GNWT) facilitated field work. De Beers (formerly Peregrine Diamonds Ltd) and Mountain Province Diamonds (formerly Kennady Diamonds) provided access to DO-18 and Kelvin kimberlite deposits, respectively.

Author Contributions

SAC and PAW conceived and designed the research. BPIP, APW and EMC collected samples. APW and EMC mapped the surface environment and APW, EMC, and BPIP interpreted results from soil geochemistry. RLS conducted microbial community analyses. BPIP analysed the surface expression of microbial anomalies. RLS, BPIP, PAW, and SAC analysed and interpreted data. SAC, PAW, and CJRH supervised research. RLS wrote the manuscript with input from BPIP, CJRH, and SAC.

Competing interests

RLS, CJRH and SAC are members of a commercial entity that offers sequencing services to the mining exploration industry and others and thus declare the existence of a financial competing interest. RLS, CJRH and SAC's commercial affiliations do not alter adherence to Nature Portfolio journals' policies on sharing data and materials.

Additional information

Supplementary information is available for this paper.

Material and methods

Geologic Setting

The DO-18 kimberlite is a Group I kimberlite that is part of the Tli Kwi Cho kimberlite complex in the Lac de Gras kimberlite field of the Archaean Slave Craton in northern Canada (S-Fig. 1). It is a classic carrot-shaped kimberlite primarily composed of pyroclastic kimberlite (PK), with less dominant phases of re-sedimented volcaniclastic kimberlite (RVK), that intruded into undifferentiated Archaean granitoids [49-51]. Sedimentary mudstones and terrestrial palynomorphs that infill the kimberlite constrain the age emplacement to between 75 Ma and 45 Ma (Late Cretaceous to Eocene) at the northernmost stand of the Western Interior Seaway [51]. DO-18 is concealed by 5-20 m of glacial till that was deposited during the most recent late Wisconsinan glaciation by westward flow (290°- 295°) [52, 53]. The DO-18 kimberlite has an expression of 4 ha at the till-bedrock interface [51].

The Kelvin kimberlite is also hosted within the Slave Craton of northern Canada (Fig. S1), as one of four gently dipping, irregular L-shaped pipes that make up the Kelvin-Faraday Corridor (KFC) cluster [54, 55]. It is composed of eight separate kimberlite phases of early Cambrian age, that are dominantly Kimberley-type pyroclastic kimberlite (KPK) with lesser hypabyssal kimberlite (HK), hosted within metaturbidites of the Yellowknife supergroup [54, 56]. The Kelvin body is concealed under 150 m of bedrock at its northernmost extent, with the only 'outcropping' rock located beneath Kelvin Lake (0.08 ha) [54, 55]. The Kelvin kimberlite is further buried beneath a relatively thin (4 m) till blanket that was glacially deposited in the late Wisconsinan, with the most recent direction of glacial flow at 268° [57].

296 *Geochemical Profiles*

297 Traditional surface-based geochemical techniques for kimberlite exploration have historically been
298 employed by identifying geochemical signatures down-ice from kimberlites through various near-total
299 acid soil digestions. However, geochemical gradients of pathfinder elements when exploring for
300 kimberlites can be too subtle for reliable detection. A suite of indicator and pathfinder elements from these
301 analyses are typically utilized to find buried targets including Ni, Cr, Ba, Co, Sr, Rb, Nb, Mg, Ta, Ca, Fe,
302 K, Ti, and rare-earth elements (REEs), but their application depends on understanding the wide range of
303 kimberlite host rock compositions. At DO-18 and Kelvin, anomalous concentrations of Cr, Ni, Nb and
304 Mg were found to be best spatially associated with the down-ice distribution of kimberlite materials in till
305 (S-Fig. 2 and S-Fig. 3). A sum of Cr, Ni, Nb, Mg concentrations (S-Fig. 2 and S-Fig. 3) to a non-parametric
306 normalized scale enhances the signal giving increased confidence in the likelihood of a subsurface
307 kimberlite. The primary elements at DO-18 and Kelvin are controlled by the weathering of dominant
308 minerals during clastic dispersion including olivine ($(Mg,Fe)_2SiO_4$), chromite ($FeCr_2O_4$), pyrope
309 ($Mg_3Al_2Si_3O_{12}$) and picroilmenite ($FeTiO_3$) for Cr; olivine; picroilmenite and pyrope for Mg;
310 picroilmenite for Nb; and olivine, picroilmenite and chromite for Ni. At both Kelvin and DO-18,
311 geochemical anomalies in Cr, Ni, Nb, Mg in till generated by mechanical glacial dispersion are
312 concentrated in the down-ice direction (S-Fig. 2 and S-Fig. 3) and to lesser extent above the kimberlite.
313 This technique allows for vectoring towards a potential kimberlite via mineral and element trains in till
314 but does not typically delineate the target directly.

315

316 *Field Sampling and QA/QC*

317 Soils for microbial-community analysis at DO-18 and Kelvin were sampled with sanitized equipment
318 without field screening, to preserve the microbial community as much as possible. Descriptions were

documented for in situ physicochemical variables at each sample site for every observed soil horizon in the profile. Soils at the field sites are derived from the breakdown of till by surface-weathering processes in situ, so the soils are considered residual weathering products of the till blanket. The B-horizon soils were targeted for microbial soil samples, although multiple horizons (including O, Ah, Ae, and C) were taken, where possible, for future analyses. Microbial soil samples were frozen at –20° C upon return to the laboratory at The University of British Columbia (UBC) after 1-2 weeks in field storage and transit, prior to DNA extraction. Soil samples were also collected for geochemical analysis. Field measurements consisted of slurry tests for pH and oxidation-reduction potential (ORP) after field sieving to below 180µm. Geochemical samples (~1 kg) were sent to ALS Minerals Laboratories Ltd. (North Vancouver, BC) for multi-acid digestion and subsequent analysis via ICP-MS. Field duplicates, CRMs (certified reference materials), and blanks were inserted into the analytical stream every 15 samples.

Kimberlite Amendment Soil Incubation Experiments

A bulk soil sample from the Kelvin area with background-level metal concentrations was collected from the upper B-horizon under aseptic conditions. The soil was packed into a sealed Poly Ore sample bag and stored at ambient temperature in the field. The soil was digested using a multi-acid near total digestion and the digestate analysed by inductively coupled plasma–mass spectrometry (ICP-MS) to determine that the soil contained 15 ppm Cr, 0.24 % Mg, 7 ppm Ni, and 2 ppm Nb. The bulk soil was not dried prior to the start of the experiment. We amended tundra-derived soils with pulverized kimberlite (80% passing 10 mesh (2 mm)). Soil was dispensed aseptically into sterile containers for each treatment with amendment concentrations chosen to represent concentrations of pathfinder elements that are routinely detected in geochemical surveys over buried mineral deposits (5% dilution). Soil was sampled at T = 0, T = 1 (15 days), T = 2 (55 days), and T=3 (85 days).

342

343 *DNA Extraction and QA/QC*

344 DNA was extracted using a DNeasy PowerSoil Kit (Qiagen). Resulting DNA was stored at -20 C. DNA
345 was quantified using the PicoGreen® Assay (Invitrogen) for dsDNA and measured on a TECAN™ M200
346 (excitation at 480 nm and emission at 520 nm). The purity and quality of the extracted DNA was assessed
347 based on the ratio of absorbance at 260 nm to absorbance at 280 nm, which were measured using a
348 NanoDrop® ND-1000 spectrophotometer (Thermo Scientific).

349

350 *SSU rRNA gene Amplification and DNA Amplicon Sequencing*

351 Bacterial and archaeal SSU rRNA gene fragments (V4 region) were amplified from the extracted genomic
352 DNA using primers 515F and 806R. Sample preparation for amplicon sequencing was performed as
353 described in [37] and [58]. In brief, the aforementioned SSU rRNA gene-targeting primers, complete with
354 Illumina adapter, an 8-nt index sequence, a 10-nt pad sequence, a 2-nt linker and the gene specific primer
355 were used in equimolar concentrations of 0.2µm together with dNTPs, PCR buffer, MgCl2, 2U/ul
356 ThermoFisher Phusion Hot Start II DNA polymerase, and PCR-certified water to a final volume of 25 L.
357 PCR amplification was performed with an initial denaturing step of 95 C for 2 min, followed by 30 cycles
358 of denaturation (95 C for 30 s), annealing (55 C for 30 s), and elongation (72 C for 1 min), with a final
359 elongation step at 72 C for 10 min. Equimolar concentrations of prepared amplicon bearing solutions were
360 pooled into a single library by using the Invitrogen SequalPrep kit. The amplicon library was analysed on
361 an Agilent Bioanalyser using the High Sensitivity dsDNA assay to determine approximate library
362 fragment size, and to verify library integrity. Pooled library DNA concentration was determined using the
363 KAPA Library Quantification Kit for Illumina. Library pools were diluted to 4 nM DNA, which was
364 denatured into single strands using fresh 0.2 N NaOH, as recommended by Illumina. The final library was

365 loaded at a concentration of 8 pM DNA, with an additional PhiX spike-in of 5 – 20%. Sequencing was
366 conducted with MiSeq at the UBC sequencing centre.
367
368 *Bioinformatics*
369 DNA sequences were processed using the Mothur amplicon sequence analysis pipeline [59]. Sequences
370 were removed from the analysis if they contained ambiguous characters, had homopolymers longer than
371 8 bp, or did not align to a reference alignment of the sequencing region. Unique sequences and their
372 frequencies in each sample were identified and then a pre-clustering algorithm was used to further de-
373 noise sequences within each sample [60]. The unique sequences were aligned against the SILVA reference
374 alignment (available online at https://mothur.org/wiki/silva_reference_files/). Sequences were chimera
375 checked using vsearch [61, 62] and reads were then clustered into 97% OTUs using OptiClust [63]. OTUs
376 were classified using SILVA reference taxonomy database (release 132, available online at
377 https://mothur.org/wiki/silva_reference_files/). OTUs that had less than 2 reads were filtered from
378 analysis. For alpha and beta diversity measures, all samples were subsampled to the lowest coverage
379 depth 16365 and calculated in Mothur [59]. Sequences were deposited into the Sequence read archive
380 (SRA) under accession number PRJNA698256
381
382 *Anomaly Identification and Mapping*
383 Indicator species analyses were performed based on algorithms defined by [64] where indicator species
384 (OTUs) are considered significant if the LDA score > 2. Sample groups for the kimberlite amendment
385 incubation experiment are based on unamended “control soils” and amended “kimberlite-bearing soils”.
386 Sample groups were set for field analyses based on their origin from “background soil” or “soils above
387 kimberlite”. These groups are defined based on underlying geology whereby “background soils” come

388 from above the metaturbidite (Kelvin) or granodiorite (DO-18) host rock and "soils above kimberlite"
389 come from above the surface projection of the kimberlites as defined by drilling.
390
391 Incubation-derived LEfSe indicator species showing an enrichment in the kimberlite amended soil
392 samples were curated to plot at DO-18. Indicator species with > 1 average reads per sample in the
393 incubation experiment and positive response ratios at the DO-18 field site were included. Response ratios
394 for indicator species were calculated as the ratio between the average relative abundance in "soils above
395 kimberlite" and the average relative abundance of "background soils". LEfSe indicator species predicted
396 from the DO-18 and Kelvin field sites were not curated further, thus each indicator species output was
397 included in the generation of the anomaly maps.
398
399 Map data plots were created using relative abundances of indicator species from 16SrRNA sequencing
400 and pathfinder element concentrations from 4-acid digest ICP-MS results. Individual indicator species and
401 pathfinder elements were normalized to the mean prior to summation. Response ratio bar plots of the
402 normalized sums of indicator species and pathfinder elements are expressed by the following equation:
403 $\left(\left(average\left(\frac{\text{on deposit}}{\text{off deposit}}\right)\right)-1\right)*100$. Anomaly identification through probability plots was done in the
404 Reflex/Imdex ioGas software, and mapping of anomalies and surficial geology was performed in the ESRI
405 ArcGIS software. To determine if predictive indicators could be generated by chance, we randomized
406 the sample group sets for field analyses based on their origin from "background soil" or "soils above
407 kimberlite". Response ratios at the Kelvin field site were calculated based on a set of 10 randomly
408 generated Lefse results from DO-18 (Table S7). Seven of ten of these response ratios were negative
409 showing no spatial correlation between the bacterial anomaly and the surface projection of the Kelvin

kimberlite. This shows that it is unlikely that our collection of indicator species, which display positive surface anomalies with respect to subsurface kimberlites, could be randomly generated.

References

1. Falkowski, P.G., T. Fenchel, and E.F. Delong, *The microbial engines that drive Earth's biogeochemical cycles.* science, 2008. **320**(5879): p. 1034-1039.
2. Newman, D.K. and J.F. Banfield, *Geomicrobiology: How molecular-scale interactions underpin biogeochemical systems.* Science, 2002. **296**(5570): p. 1071-1077.
3. Oltvai, Z.N. and A.-L. Barabási, *Life's complexity pyramid.* Science, 2002. **298**(5594): p. 763-764.
4. Green, J.L., B.J. Bohannan, and R.J. Whitaker, *Microbial biogeography: from taxonomy to traits.* science, 2008. **320**(5879): p. 1039-1043.
5. Martiny, J.B.H., et al., *Microbial biogeography: putting microorganisms on the map.* Nature Reviews Microbiology, 2006. **4**(2): p. 102-112.
6. Becking, L.G.M.B., *Geobiologie of inleiding tot de milieukunde*. 1934: WP Van Stockum & Zoon.
7. Smith, M.B., et al., *Natural bacterial communities serve as quantitative geochemical biosensors.* MBio. **6**(3): p. e00326-15.
8. Gianoulis, T.A., et al., *Quantifying environmental adaptation of metabolic pathways in metagenomics.* Proceedings of the National Academy of Sciences, 2009. **106**(5): p. 1374-1379.
9. Tringe, S.G., et al., *Comparative metagenomics of microbial communities.* Science, 2005. **308**(5721): p. 554-557.
10. Lauber, C.L., et al., *Pyrosequencing-based assessment of soil pH as a predictor of soil bacterial community structure at the continental scale.* Applied and environmental microbiology, 2009. **75**(15): p. 5111-5120.
11. Rath, K.M., et al., *Linking bacterial community composition to soil salinity along environmental gradients.* The ISME journal, 2019. **13**(3): p. 836-846.
12. Oliverio, A.M., M.A. Bradford, and N. Fierer, *Identifying the microbial taxa that consistently respond to soil warming across time and space.* Global Change Biology, 2017. **23**(5): p. 2117-2129.
13. Luo, C., et al., *Soil microbial community responses to a decade of warming as revealed by comparative metagenomics.* Applied and environmental microbiology, 2014. **80**(5): p. 1777-1786.
14. Bryant, J.A., et al., *Wind and sunlight shape microbial diversity in surface waters of the North Pacific Subtropical Gyre.* The ISME journal, 2016. **10**(6): p. 1308-1322.
15. Tortell, P.D., et al., *Marine bacteria and biogeochemical cycling of iron in the oceans.* FEMS Microbiology Ecology, 1999. **29**(1): p. 1-11.
16. Winterburn, P.A., R.R. Noble, and D. Lawie, *Advances in exploration geochemistry, 2007 to 2017 and beyond.* Geochemistry: Exploration, Environment, Analysis, 2020. **20**(2): p. 157-166.

17. Kesler, S.E. *Mineral supply and demand into the 21st century*. in *Proceedings for a Workshop on Deposit Modeling, Mineral Resource Assessment, and Their Role in Sustainable Development. Circular*. 2007.
18. Lusty, P. and A. Gunn, *Challenges to global mineral resource security and options for future supply.* Geological Society, London, Special Publications, 2015. **393**(1): p. 265-276.
19. Cameron, E.M., et al., *Finding deeply buried deposits using geochemistry.* Geochemistry: Exploration, Environment, Analysis, 2004. **4**(1): p. 7-32.
20. Kelley, D.L., et al., *Beyond the obvious limits of ore deposits: The use of mineralogical, geochemical, and biological features for the remote detection of mineralization.* Economic Geology, 2006. **101**(4): p. 729-752.
21. Gilliss, M., et al., *Geochemical dispersion in groundwater from a weathered Cu–Zn deposit in glaciated terrain.* Geochemistry: Exploration, Environment, Analysis, 2004. **4**(4): p. 291-305.
22. Cannon, H.L., *Botanical prospecting for ore deposits.* Science, 1960. **132**(3427): p. 591-598.
23. Kruckeberg, A.R., *Geology and plant life: the effects of landforms and rock types on plants*. 2004: University of Washington Press.
24. Anand, R., M. Cornelius, and C. Phang, *Use of vegetation and soil in mineral exploration in areas of transported overburden, Yilgarn Craton, Western Australia: a contribution towards understanding metal transportation processes.* Geochemistry: Exploration, Environment, Analysis, 2007. **7**(3): p. 267-288.
25. Brooks, R.R., C.E. Dunn, and G.E. Hall, *Biological systems in mineral exploration and processing*. 1995: Pearson Prentice Hall.
26. Brooks, R., *Indicator plants for mineral prospecting—a critique.* Journal of Geochemical Exploration, 1979. **12**: p. 67-78.
27. Greig-Smith, P., *Pattern in vegetation.* Journal of Ecology, 1979. **67**(3): p. 755-779.
28. Grime, J.P., *Plant strategies, vegetation processes, and ecosystem properties*. 2006: John Wiley & Sons.
29. Reith, F. and S. Rogers, *Assessment of bacterial communities in auriferous and non-auriferous soils using genetic and functional fingerprinting.* Geomicrobiology Journal, 2008. **25**(3-4): p. 203-215.
30. Wakelin, S., et al., *Assessing microbiological surface expression over an overburden-covered VMS deposit.* Journal of Geochemical Exploration, 2012. **112**: p. 262-271.
31. Leslie, K., et al., *Marinobacter bacteria associated with a massive sulphide ore deposit affect metal mobility in the deep subsurface.* Geochemistry: Exploration, Environment, Analysis, 2015. **15**(4): p. 319-326.
32. Leslie, K., et al., *Biogeochemical controls on metal mobility: modeling a Cu-Zn VMS deposit in column flow-through studies.* Geochemistry: Exploration, Environment, Analysis, 2014. **14**(1): p. 59-70.
33. Leslie, K., et al., *Biogeochemical indicators of buried mineralization under cover, Talbot VMS Cu–Zn prospect, Manitoba.* Applied geochemistry, 2013. **37**: p. 190-202.
34. Fierer, N. and R.B. Jackson, *The diversity and biogeography of soil bacterial communities.* Proceedings of the National Academy of Sciences, 2006. **103**(3): p. 626-631.
35. Anderson, I.C. and J.W. Cairney, *Diversity and ecology of soil fungal communities: increased understanding through the application of molecular techniques.* Environmental microbiology, 2004. **6**(8): p. 769-779.

36. McCaig, A.E., L.A. Glover, and J.I. Prosser, *Numerical analysis of grassland bacterial community structure under different land management regimens by using 16S ribosomal DNA sequence data and denaturing gradient gel electrophoresis banding patterns.* Applied and environmental microbiology, 2001. **67**(10): p. 4554-4559.
37. Caporaso, J.G., et al., *Global patterns of 16S rRNA diversity at a depth of millions of sequences per sample.* Proceedings of the national academy of sciences, 2011. **108**(Supplement 1): p. 4516-4522.
38. Delgado-Baquerizo, M., et al., *A global atlas of the dominant bacteria found in soil.* Science, 2018. **359**(6373): p. 320-325.
39. Thompson, L.R., et al., *A communal catalogue reveals Earth's multiscale microbial diversity.* Nature, 2017. **551**(7681): p. 457-463.
40. Xiong, W., et al., *A global overview of the trophic structure within microbiomes across ecosystems.* Environment International, 2021. **151**: p. 106438.
41. Fierer, N., *Embracing the unknown: disentangling the complexities of the soil microbiome.* Nature Reviews Microbiology, 2017. **15**(10): p. 579-590.
42. Bahram, M., et al., *Metagenomic assessment of the global diversity and distribution of bacteria and fungi.* Environmental Microbiology, 2021. **23**(1): p. 316-326.
43. Mervine, E.M., et al., *Potential for offsetting diamond mine carbon emissions through mineral carbonation of processed kimberlite: an assessment of De Beers mine sites in South Africa and Canada.* Mineralogy and Petrology, 2018. **112**(2): p. 755-765.
44. Zeyen, N., et al., *Mineral carbonation at Venetia and Gahcho Kué diamond mines: Characterization of the highly reactive clay fraction.* Goldschmidt2021• Virtual• 4-9 July, 2021.
45. Johnston, E.R., et al., *Responses of tundra soil microbial communities to half a decade of experimental warming at two critical depths.* Proceedings of the National Academy of Sciences, 2019. **116**(30): p. 15096-15105.
46. Hale, L., et al., *Tundra microbial community taxa and traits predict decomposition parameters of stable, old soil organic carbon.* The ISME journal, 2019. **13**(12): p. 2901-2915.
47. Frank-Fahle, B.A., et al., *Microbial functional potential and community composition in permafrost-affected soils of the NW Canadian Arctic.* PLoS One, 2014. **9**(1): p. e84761.
48. Carini, P., et al., *Relic DNA is abundant in soil and obscures estimates of soil microbial diversity.* Nature microbiology, 2016. **2**(3): p. 1-6.
49. Doyle, B., K. Kivi, and B.S. Smith. *The Tli Kwi Cho (DO27 and DO18) Diamondiferous Kimberlite Complex Slave Craton, Northwest Territories, Canada*. in *International Kimberlite Conference: Extended Abstracts*. 1998.
50. Eggleston, T., K. Brisebois, and J. Pell, *Lac de Gras project northwest territories.* Canada: NI, 2014: p. 43-101.
51. Harder, M., et al. *The preliminary geology of the DO-18 kimberlite, Lac de Gras kimberlite province, Canada*. in *International Kimberlite Conference: Extended Abstracts*. 2008.
52. Dredge, L., B. Ward, and D. Kerr, *Glacial geology and implications for drift prospecting in the Lac de Gras, Winter Lake, and Aylmer Lake map areas, central Slave Province, Northwest Territories.* Current research, 1994: p. 33-38.
53. Ward, B., et al., *Kimberlite indicator minerals in glacial deposits, Lac de Gras area, NWT*. 1996.
54. Bezzola, M., et al., *Geology and resource development of the Kelvin kimberlite pipe, Northwest Territories, Canada.* Mineralogy and Petrology, 2018. **112**(2): p. 463-475.

55. Vivian, G. and T. Nowicki, *Kennady North Project. Technical report.* Aurora Geosciences, 2016.
56. Smith, B.S., et al. *Kimberlite terminology and classification*. in *Proceedings of 10th international kimberlite conference*. 2013. Springer.
57. Knight, J., *An interpretation of the deglaciation history of the southern Slave Province using 1:50 000 surficial geology maps. .* Northwest Territories Geological Survey, Open Report 2017-018, 2018.
58. Apprill, A., et al., *Minor revision to V4 region SSU rRNA 806R gene primer greatly increases detection of SAR11 bacterioplankton.* Aquatic Microbial Ecology, 2015. **75**(2): p. 129-137.
59. Schloss, P.D., et al., *Introducing mothur: open-source, platform-independent, community-supported software for describing and comparing microbial communities.* Applied and environmental microbiology, 2009. **75**(23): p. 7537-7541.
60. Schloss, P.D., D. Gevers, and S.L. Westcott, *Reducing the effects of PCR amplification and sequencing artifacts on 16S rRNA-based studies.* PloS one, 2011. **6**(12): p. e27310.
61. Edgar, R.C., *Search and clustering orders of magnitude faster than BLAST.* Bioinformatics, 2010. **26**(19): p. 2460-2461.
62. Rognes, T., et al., *VSEARCH: a versatile open source tool for metagenomics.* PeerJ, 2016. **4**: p. e2584.
63. Westcott, S.L. and P.D. Schloss, *OptiClust, an improved method for assigning amplicon-based sequence data to operational taxonomic units.* mSphere, 2017. **2**(2): p. e00073-17.
64. Segata, N., et al., *Metagenomic biomarker discovery and explanation.* Genome biology, 2011. **12**(6): p. 1-18.

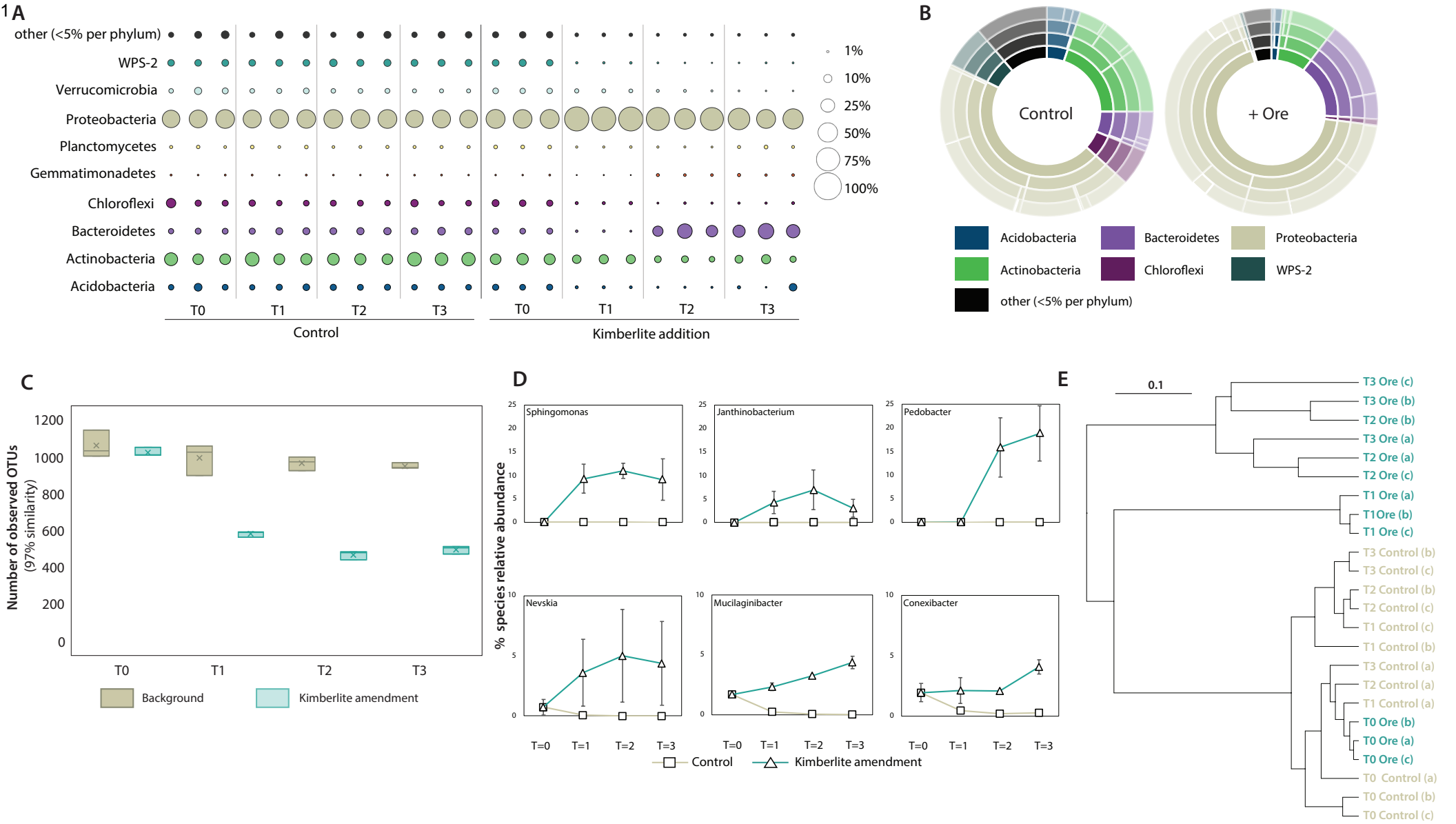
A
other (<5% per phylum)
WPS-2
Verrucomicrobia
Proteobacteria
Planctomycetes
Gemmatimonadetes
Chloroflexi
Bacteroidetes
Actinobacteria
Acidobacteria
T0
T1
T2
T3
Control
Kimberlite addition
1%
10%
25%
50%
75%
100%
B
Control
+ Ore
Acidobacteria
Actinobacteria
other (<5% per phylum)
Bacteroidetes
Chloroflexi
Proteobacteria
WPS-2
C
Number of observed OTUs
(97% similarity)
Background
Kimberlite amendment
D
% species relative abundance
Sphingomonas
Janthinobacterium
Pedobacter
Nevskia
Mucilaginibacter
Conexibacter
T=0
T=1
T=2
T=3
Control
Kimberlite amendment
E
0.1
T3 Ore (c)
T3 Ore (b)
T2 Ore (b)
T3 Ore (a)
T2 Ore (a)
T2 Ore (c)
T1 Ore (a)
T1Ore (b)
T1 Ore (c)
T3 Control (b)
T3 Control (c)
T2 Control (b)
T2 Control (c)
T1 Control (c)
T1 Control (b)
T3 Control (a)
T2 Control (a)
T1 Control (a)
T0 Ore (b)
T0 Ore (a)
T0 Ore (c)
T0 Control (a)
T0 Control (b)
T0 Control (c)

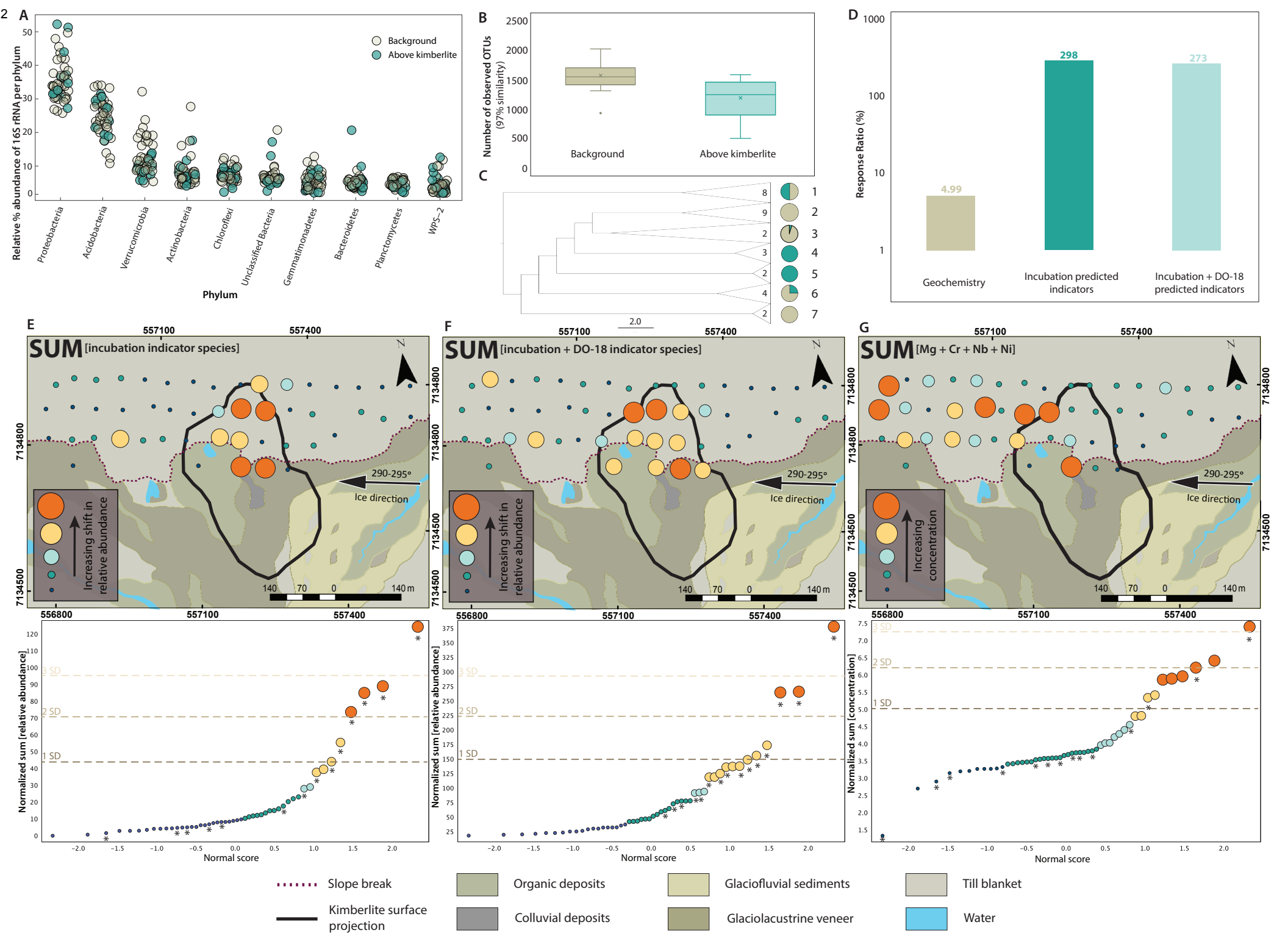
2
A
Relative % abundance of 16S rRNA per phylum
Background
Above kimberlite
Proteobacteria
Acidobacteria
Verrucomicrobia
Actinobacteria
Chloroflexi
Unclassified Bacteria
Gemmatimonadetes
Bacteroidetes
Planctomycetes
WPS–2
Phylum
B
Number of observed OTUs (97% similarity)
Background
Above kimberlite
C
2.0
D
Response Ratio (%)
4.99
298
273
Geochemistry
Incubation predicted indicators
Incubation + DO-18 predicted indicators
E
SUM [incubation indicator species]
F
SUM [incubation + DO-18 indicator species]
G
SUM [Mg + Cr + Nb + Ni]
290-295°
Ice direction
Increasing shift in relative abundance
Increasing concentration
140 70 0 140 m
Normalized sum [relative abundance]
Normalized sum [concentration]
Normal score
1 SD
2 SD
3 SD
Slope break
Kimberlite surface projection
Organic deposits
Colluvial deposits
Glaciofluvial sediments
Glaciolacustrine veneer
Till blanket
Water

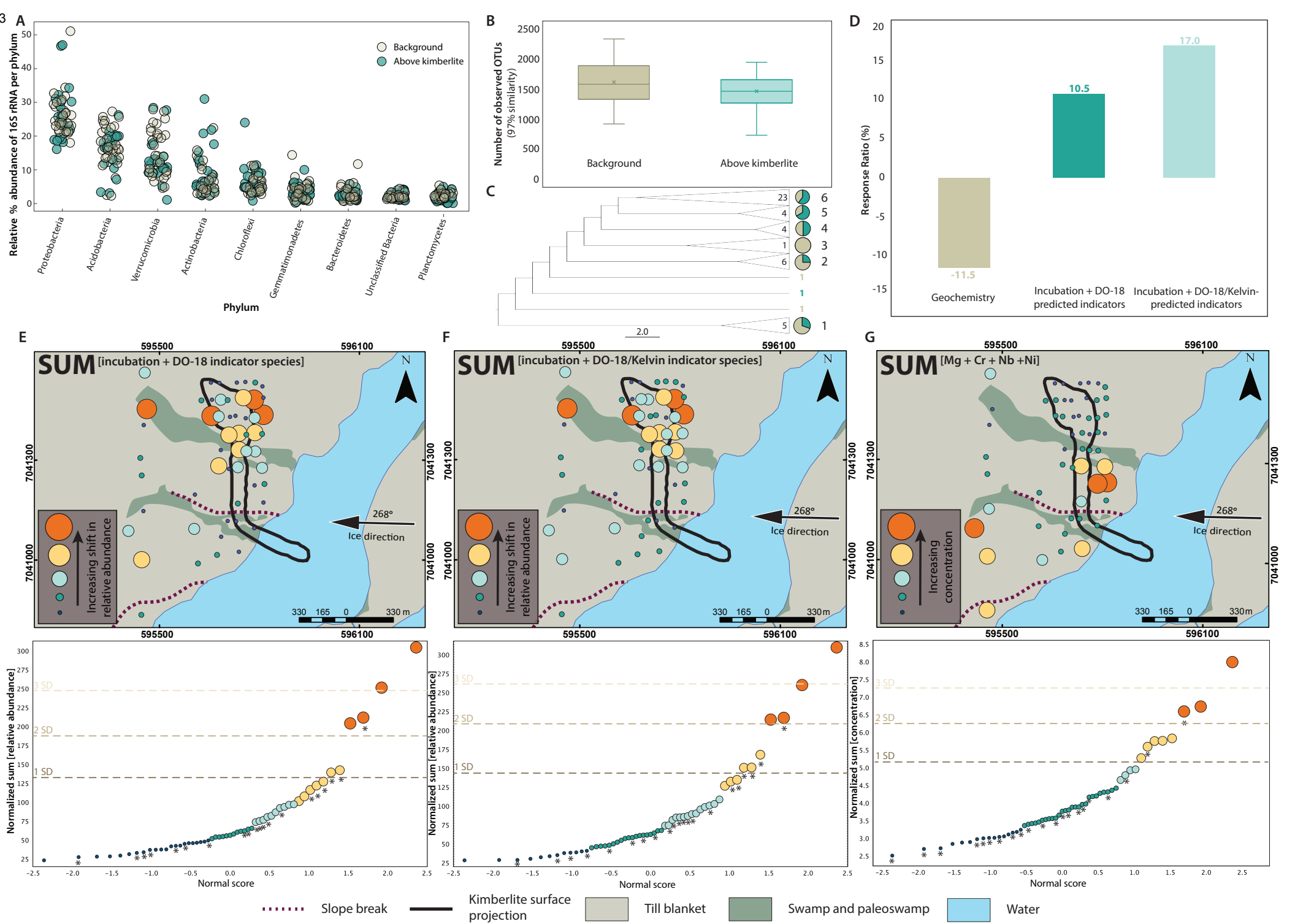
A
Relative % abundance of 16S rRNA per phylum
Background
Above kimberlite
Proteobacteria
Acidobacteria
Verrucomicrobia
Actinobacteria
Chloroflexi
Gemmatimonadetes
Bacteroidetes
Unclassified Bacteria
Planctomycetes
Phylum
B
Number of observed OTUs (97% similarity)
Background
Above kimberlite
C
2.0
D
Response Ratio (%)
-11.5
10.5
17.0
Geochemistry
Incubation + DO-18 predicted indicators
Incubation + DO-18/Kelvin-predicted indicators
E
SUM [incubation + DO-18 indicator species]
Increasing shift in relative abundance
268°
Ice direction
330 165 0 330 m
F
SUM [incubation + DO-18/Kelvin indicator species]
Increasing shift in relative abundance
268°
Ice direction
330 165 0 330m
G
SUM [Mg + Cr + Nb +Ni]
Increasing concentration
268°
Ice direction
330 165 0 330m
595500
596100
7041300
7041000
N
Normalized sum [relative abundance]
Normalized sum [concentration]
Normal score
3 SD
2 SD
1 SD
Slope break
Kimberlite surface projection
Till blanket
Swamp and paleoswamp
Water

Legends

Figure 1: Soil microbial community composition, diversity, and indicator species for the kimberlite amendment experiment.

Figure 1A. Distribution of 16S rRNA reads per phylum for each sample. The number of reads per phylum is calculated as a percentage of the total reads for each sample. The '*other' grouping represents summed phyla that individually contributed <5% of the total number of reads per sample.

Figure 1B. Sunburst chart showing the average total relative abundance of bacteria and archaeal communities in (i) control samples and (ii) ore amended samples. Rings are ordered as follows from inner to outer: Phyla, Classes, Orders, Families and Generas.

Figure 1C. Number of OTUs per sample coloured by sample treatment (from data that has been rarefied to 16365 sequences per sample). Median values are indicated by the solid line within each box, and the box extends to upper and lower quartile values.

Figure 1D. Examples of operational taxonomic unit (OTU) 'species level' changes across treatments, over time.

Figure 1E. Hierarchical relationships among samples based on Euclidean distance of 16S-OTU abundances. The hierarchical relationships between samples were obtained using the unweighted pair group method with arithmetic mean (UPGMA) clustering algorithm. Node labels indicate the sample/treatment.

Figure 2: Soil microbial community composition, diversity, and indicator species for the DO-18 kimberlite.

Figure 2A. Distribution of 16S rRNA reads per phylum for each sample at the DO-18 kimberlite. The number of reads per phylum is calculated as a percentage of the total reads for each sample.

Figure 2B. Number of OTUs per sample coloured by sample origin (from data that has been rarefied to 16365 sequences per sample). Median values are indicated by the solid line within each box, and the box extends to upper and lower quartile values.

Figure 2C. Hierarchical relationships among samples based on Euclidean distance of 16S-OTU abundances. The hierarchical relationships between samples were obtained using the unweighted pair group method with arithmetic mean (UPGMA) clustering algorithm. Node labels indicate the sample/treatment. Pie charts indicate the % of samples that are located on deposit (blue segments) and % of sample that located off deposit (beige segments).

Figure 2D. Response ratios of geochemical pathfinder elements compared to suites of indicator species derived from microbial community fingerprinting at DO-18. Response ratios are expressed in percent calculated by the average "on deposit" over the average "off deposit" relative to an equivalent ratio of 1.

Figure 2E. Microbial anomaly map showing the normalized sum of incubation predicted indicator species' spatial distribution at DO-18. Indicator species are based on a LEfSe indicator species analysis. Individual indicator species are normalized by the mean prior to summation and anomaly intervals are based on probability plots.

Figure 2F. Microbial anomaly map showing the normalized sum of incubation predicted indicator species and DO-18 predicted indicator species' spatial distribution at DO-18. Indicator species are

based on a LEfSe indicator species analysis. Individual indicator species are normalized by the mean prior to summation and anomaly intervals are based on probability plots.

Figure 2G. Geochemical anomaly map at DO-18 showing the normalized sum of pathfinder elements Cr, Mg, Nb, and Ni. Results are derived from 4-acid digests and ICP-MS of b-horizon soils. Each pathfinder element was normalized to the mean prior to summation and anomaly intervals are based on probability plots. Data overlies a surficial materials map. In each map (E, F, G), data overlies a surficial materials map and the "*" on the probability plots represents samples that correspond spatially to "on deposit".

Figure 3: Soil microbial community composition, diversity, and indicator species for the Kelvin kimberlite.

Figure 3A. Distribution of 16S rRNA reads per phylum for each sample at the Kelvin kimberlite. The number of reads per phylum is calculated as a percentage of the total reads for each sample.

Figure 3B. Number of OTUs per sample coloured by sample origin (from data that has been rarefied to 16365 sequences per sample). Median values are indicated by the solid line within each box, and the box extends to upper and lower quartile values.

Figure 3C. Hierarchical relationships among samples based on Euclidean distance of 16S-OTU abundances. The hierarchical relationships between samples were obtained using the unweighted pair group method with arithmetic mean (UPGMA) clustering algorithm. Node labels indicate the sample/treatment. Pie charts indicate the % of samples that are located on deposit (blue segments) and % of sample that located off deposit (beige segments).

Figure 3D. Response ratios of geochemical pathfinder elements compared to suites of indicator species derived from microbial community fingerprinting at Kelvin. Response ratios are expressed

in percent calculated by the average “on deposit” over the average “off deposit” relative to an equivalent ratio of 1.

Figure 3E. Microbial anomaly map showing the normalized sum of incubation predicted indicator species and DO-18 predicted indicator species’ spatial distribution at Kelvin. Indicator species are based on a LEfSe indicator species analysis. Individual indicator species are normalized by the mean prior to summation and anomaly intervals are based on probability plots.

Figure 3F. Microbial anomaly map showing the normalized sum of incubation predicted indicator species, DO-18 predicted indicator species, and Kelvin predicted indicator species’ spatial distribution at Kelvin. Indicator species are based on a LEfSe indicator species analysis. Individual indicator species are normalized by the mean prior to summation and anomaly intervals are based on probability plots.

Figure 3G. Geochemical anomaly map at DO-18 showing the normalized sum of pathfinder indicator elements Cr, Mg, Nb, and Ni. Results are derived from 4-acid digests and ICP-MS of b-horizon soils. Each pathfinder element was normalized to the mean prior to summation and anomaly intervals are based on probability plots. In each map (E, F, G), data overlies a surficial materials map and the “*” on the probability plots represents samples that correspond spatially to “on deposit”.